JACS
JOURNAL OF THE AMERICAN CHEMICAL SOCIETY
Communication
pubs.acs.org/JACS

The NiCEST Approach: Nickel(II) ParaCEST MRI Contrast Agents

Abiola O. Olatunde,[†] Sarina J. Dorazio,[†] Joseph A. Spernyak,[§] and Janet R. Morrow*[,†]

[†]Department of Chemistry, University at Buffalo, State University of New York, Amherst, New York 14260, United States
[§]Department of Cell Stress Biology, Roswell Park Cancer Institute, Buffalo, New York 14263, United States

Supporting Information

ABSTRACT: Paramagnetic Ni(II) complexes are shown here to form paraCEST MRI contrast agents (paraCEST = paramagnetic chemical exchange saturation transfer; NiCEST = Ni(II) based CEST agents). Three azamacrocycles with amide pendent groups bind Ni(II) to form stable NiCEST contrast agents including 1,4,7-tris(carbamoylmethyl)-1,4,7-triazacyclononane (**L1**), 1,4,8,11-tetrakis(carbamoylmethyl)-1,4,8,11-tetraazacyclotetradecane (**L2**), and 7,13-bis(carbamoylmethyl)-1,4,10-trioxa-7,13-diazacyclopentadecane (**L3**). $[Ni(\mathbf{L3})]^{2+}$, $[Ni(\mathbf{L1})]^{2+}$, and $[Ni(\mathbf{L2})]^{2+}$ have CEST peaks attributed to amide protons that are shifted 72, 76, and 76 ppm from the bulk water resonance, respectively. Both CEST MR images and CEST spectroscopy show that $[Ni(\mathbf{L3})]^{2+}$ has the largest CEST effect in 100 mM NaCl, 20 mM HEPES pH 7.4 at 37 °C. This larger CEST effect is attributed to the sharper proton resonances of the complex which arise from a rigid structure and low relaxivity.

One of the greatest challenges in the design of effective paraCEST MRI contrast agents is the selection of a paramagnetic metal ion. The paramagnetic center must produce highly shifted yet relatively narrow proton resonances and at least one of these highly shifted protons must be in chemical exchange with water. Irradiation at the resonant frequency of the exchangeable proton saturates the magnetization and, upon exchange, reduces the intensity of the bulk water proton resonance.[1] To date, Ln(III) ions, especially Eu(III), Yb(III), and Tm(III), have been the paramagnetic metal ions of choice because complexes of these ions provide the best compromise between large chemical shift dispersion and narrow line widths.[1] As an alternative to Ln(III) contrast agents, we recently reported the first example of a macrocyclic Fe(II) paraCEST contrast agent.[2−4] Transition metal ions have the dual advantage of very versatile coordination chemistry and a more substantial contact (through-bond) contribution to paramagnetic shifts compared to Ln(III) ions.[5] Here we report the first Ni(II) macrocyclic complexes that are paraCEST MRI contrast agents. Similar to Fe(II), the key to forming successful paraCEST agents for Ni(II) is control of spin state, metal ion dissociation kinetics and fluxionality of the macrocyclic complex on the NMR time scale. However, stabilizing the divalent oxidation state under biologically relevant conditions is more straightforward for Ni(II) than for Fe(II).

The Ni(II) ion has relatively short electronic relaxation time constants (T_{1e}) that produce highly shifted and, in some cases, narrow proton resonances. Tetrahedral and bipyramidal Ni(II) complexes tend to have shorter T_{1e} and correspondingly sharper proton resonances than do octahedral complexes.[5−9] To probe different coordination geometries, three Ni(II) complexes were studied (Chart 1). $[Ni(\mathbf{L1})]^{2+}$ forms a six-coordinate complex with a twisted trigonal antiprismatic geometry.[10] $[Ni(\mathbf{L2})]^{2+}$ also is most likely a six-coordinate complex, as the tetracarboxylate analogue of **L2** exhibits four bound amino groups and two bound pendent amide donor groups.[11] By contrast, $[Ni(\mathbf{L3})]^{2+}$ is likely to be a seven-coordinate pentagonal bipyramidal complex with the oxygen and nitrogen donors of the macrocycle forming the pentagonal base and the two pendent groups capping the axial sites, similar to that observed for a Ni(II) complex of an analogous macrocycle containing two benzimidazole pendents.[12,13] In aqueous solution, the effective magnetic moments of $[Ni(\mathbf{L1})]^{2+}$, $[Ni(\mathbf{L2})]^{2+}$, and $[Ni(\mathbf{L3})]^{2+}$ at 25 °C are 3.2, 3.1, and 3.4 μ_B, consistent with high spin Ni(II) (eq S2 in Supporting Information).

Chart 1. Structures of Ni(II) Complexes

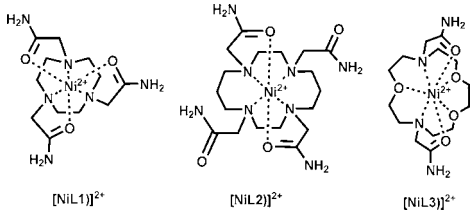

The appearance of the paramagnetic ^{1}H NMR spectra of the three complexes is quite different (Figures S1−S3). $[Ni(\mathbf{L3})]^{2+}$ shows 12 distinct nonexchangeable proton resonances of equal intensity and two distinct exchangeable NH protons, consistent with a complex of apparent C_2 symmetry in CD_3CN. The amide NH protons are identified by their disappearance upon addition of a few drops of D_2O. Similar to Fe(II) amide complexes,[3,14] the two chemically inequivalent amide NH proton resonances have a large chemical shift difference (82 and 16 ppm). All proton resonances are quite sharp, with FWHH ranging from 150 to 400 Hz. This proton NMR spectrum is consistent with a static structure on the NMR time scale. In contrast, $[Ni(\mathbf{L1})]^{2+}$ has two distinct NH amide protons in CD_3CN (83 and 14 ppm), but the remaining proton resonances are quite broad. This proton spectrum is reminiscent of that of $[Fe(\mathbf{L1})]^{2+}$ which also contains relatively

Received: August 13, 2012
Published: October 27, 2012

   dx.doi.org/10.1021/ja307909x | J. Am. Chem. Soc. 2012, 134, 18503−18505

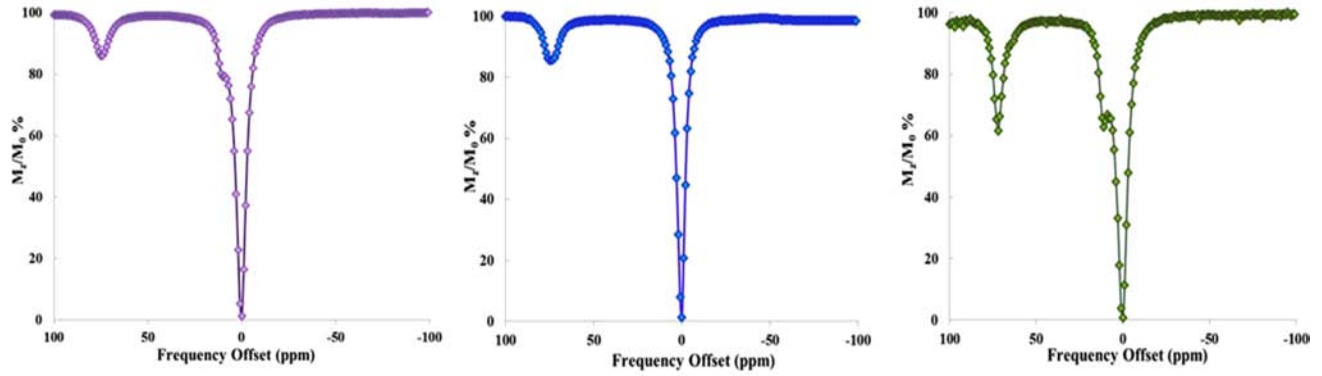

Figure 1. CEST spectra recorded at 11.7 T of a solution containing 10 mM $[Ni(\mathbf{L1})]^{2+}$ (left), 100 mM NaCl, 20 mM HEPES, pH 7.3; 10 mM $[Ni(\mathbf{L2}]^{2+}$ (middle), 100 mM NaCl, 20 mM HEPES, pH 7.4; 10 mM $[Ni(\mathbf{L3})]^{2+}$ (right), 100 mM NaCl, 20 mM HEPES, pH 7.4. RF presaturation applied for 2 s, B_1 = 24 μT at 37 °C. The large peak arises from direct irradiation of water protons, set to 0 ppm.

sharp amide NH proton resonances and extremely broad macrocycle proton resonances.[3] The broad resonances are consistent with the fluxional nature of the transition metal ion macrocyclic complexes on the NMR time scale, presumably in a process that interconverts between diastereomeric forms that differ in pendent group and macrocycle backbone arrangement.[4] The $[Ni(\mathbf{L2})]^{2+}$ complex also has amide NH proton resonances that are more narrow than those of the macrocycle backbone. $[Ni(\mathbf{L2})]^{2+}$ is most likely six coordinate with two bound amide pendents and two unbound pendents.[11] The proton NMR of this complex in CD_3CN shows three amide proton resonances that are slightly shifted downfield from the diamagnetic region of the proton NMR spectrum at 6, 14, and 19 ppm. In addition, there is at least one highly shifted amide proton resonance at 84 ppm and possibly a second one at 80 ppm in CD_3CN that decrease in intensity upon addition of D_2O. The number of amide proton resonances is consistent with the low symmetry of the $[Ni(\mathbf{L2})]^{2+}$ complex, but the broad nature of the proton resonances in the NMR spectrum makes it difficult to obtain further information about coordination geometry.

CEST spectra were obtained by applying a presaturation pulse in 1 ppm increments and were plotted as normalized water signal intensity (M_z/M_o %) against frequency offset (ppm). Spectra were collected at 37 °C in the presence of 20 mM buffer and 100 mM NaCl, at pH 7.3–7.4 (Figure 1). The CEST peaks of all three Ni(II) complexes clearly arise from the amide NH protons that are identified by their signature appearance as two highly separated resonances for the two chemically inequivalent protons. For $[Ni(\mathbf{L1})]^{2+}$ and $[Ni(\mathbf{L3})]^{2+}$, the two CEST peaks for the distinct amide NH can be identified as one highly shifted at 76 and 72 ppm, respectively, and one close to solvent (11 ppm). $[Ni(\mathbf{L2})]^{2+}$ shows only one broadened CEST peak at 76 ppm from bulk water. The pH dependence of the CEST peak is also consistent with amide pendent groups. The CEST effect for $[Ni(\mathbf{L1})]^{2+}$ increases from pH 6.6 to 7.5 and slightly decreases at more basic pH, consistent with base-catalyzed exchange (Figure S4). Superposition of the three CEST spectra show that $[Ni(\mathbf{L3})]^{2+}$ has the most pronounced CEST peaks by 2–3 fold (Figure S5).

To validate the observed CEST spectra of the Ni(II) complexes, CEST imaging was done on a 4.7 T scanner using a phantom array containing solutions of 2, 4, or 8 mM Ni(II) complex, 100 mM NaCl, 20 mM buffer, pH 7.4 at 37 °C. A pair of gradient echo images was acquired with a presaturation pulse either on-resonance or off-resonance of the exchangeable protons (±76 ppm for $[Ni(\mathbf{L1})]^{2+}$ and $[Ni(\mathbf{L2})]^{2+}$ or ±73 ppm for $[Ni(\mathbf{L3})]^{2+}$). The ratio between these two images is subtracted from 100% to generate a CEST image. The phantoms show that CEST increases with concentration of the Ni(II) complex over the range 2–8 mM (Figure S6). At all concentrations, $[Ni(\mathbf{L3})]^{2+}$ showed more substantial CEST images by 2–4 fold (Figures 2 and S7). The T_1 and T_2

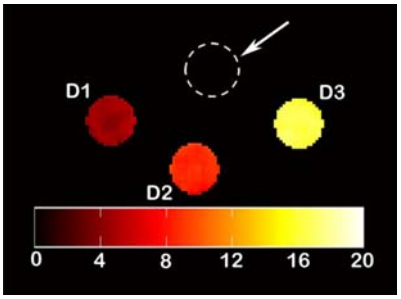

Figure 2. CEST images of phantoms on a MRI 4.7 T scanner with a pulse train comprised of five Gauss pulses at 12 μT for 1 s each, interpulse delay of 200 μs applied symmetrically about the bulk water resonance (±73 ppm) Arrow: 20 mM HEPES buffer pH 7.4 and 100 mM NaCl only. Other samples contain $[Ni(\mathbf{L3})]^{2+}$: D1 (2 mM), D2 (4 mM), D3 (8 mM) with 20 mM HEPES pH 7.4 and 100 mM NaCl at 37 °C. Scale represents the percent loss of signal due to CEST saturation pulse.

relaxivities were low for $[Ni(\mathbf{L2})]^{2+}$ (0.097 and 0.15 mM^{-1} s^{-1}) and $[Ni(\mathbf{L3})]^{2+}$ (0.012 and 0.092 mM^{-1} s^{-1}). $[Ni(\mathbf{L1})]^{2+}$ had larger relaxivities of 0.21 and 0.39 mM^{-1} s^{-1} for T_1 and T_2, respectively. The T_1 values for the Ni(II) complexes are comparable to or lower than those of Fe(II)[3] and Eu(III) complexes.[15]

It is important to consider why $[Ni(\mathbf{L3})]^{2+}$ has a larger CEST effect than do the other two complexes. For paraCEST agents with protons that are in slow exchange on the NMR time scale, the magnitude of the CEST effect is anticipated to increase with the number of chemically equivalent exchangeable protons and with increasing rate constants for proton exchange, but to decrease with greater T_1 relaxivity.[1] $[Ni(\mathbf{L3})]^{2+}$ has fewer chemically equivalent exchangeable amide protons than does $[Ni(\mathbf{L1})]^{2+}$, and rate constants for the amide proton exchange are similar for all three complexes (240–360 s^{-1}, Figure S8) suggesting that neither of these properties are responsible for

dx.doi.org/10.1021/ja307909x | J. Am. Chem. Soc. 2012, 134, 18503–18505

the larger CEST effect. However, the low T_1 relaxivity value for $[Ni(\mathbf{L3})]^{2+}$ may contribute to a greater CEST effect as it is 5−10-fold smaller than those of the other two complexes. In addition, the narrow exchangeable proton resonances of $[Ni(\mathbf{L3})]^{2+}$ are beneficial for CEST because the magnetization of these protons are more easily saturated with low pulse power. The broader NH resonances of $[Ni(\mathbf{L1})]^{2+}$ and $[Ni(\mathbf{L2})]^{2+}$ may result from longer T_{1e} and correspondingly greater proton relaxivity of these six-coordinate complexes, or alternately from the fluxional character of these complexes on the NMR time scale.

The Ni(II) complexes were examined for their resistance to dissociation in the presence of acid, metal cations and biologically relevant anions, as preliminary studies to determine suitability for *in vivo* applications. $[Ni(\mathbf{L1})]^{2+}$ and $[Ni(\mathbf{L2})]^{2+}$ were remarkably resistant to dissociation at acidic pH. No detectable dissociation was observed for $[Ni(\mathbf{L1})]^{2+}$ after incubation for 4 h at pD 1.8, 37 °C (Figures S9−11 and Table S2). $[Ni(\mathbf{L2})]^{2+}$ showed intermediate tendency to resist dissociation with 20% dissociation after 4 h. $[Ni(\mathbf{L3})]^{2+}$ was the most labile of the complexes and dissociated completely at acidic pH within 1 h. Cu(II) displacement assays showed similar results. There was no detectable dissociation of $[Ni(\mathbf{L1})]^{2+}$ or $[Ni(\mathbf{L2})]^{2+}$ upon incubation of the complexes with excess Cu(II) at 37 °C for 5 h (Figure S12). Neither did biologically relevant concentrations of phosphate (0.40 mM) and carbonate (25 mM) affect $[Ni(\mathbf{L1})]^{2+}$ or $[Ni(\mathbf{L2})]^{2+}$ as shown by a similar CEST spectrum of these complexes following incubation at 37 °C for five days (Figures S13 and S14). In contrast, $[Ni(\mathbf{L3})]^{2+}$ showed the appearance of new proton resonances upon addition of 25 mM carbonate and 0.40 mM phosphate, signifying a change in the coordination sphere by anion binding (Figure S15). Surprisingly, the CEST spectrum of the complex was not markedly changed under similar conditions (Figure S16). This suggests that the two amide pendent groups remain coordinated and relatively unaffected by the change in the coordination sphere of $[Ni(\mathbf{L3})]^{2+}$.

In conclusion, we show here that Ni(II) complexes with amide pendent groups are effective paraCEST agents with paramagnetic induced proton shifts that are similar to those of Fe(II) analogs. Ni(II) complexes of **L1** and **L2** are highly resistant to dissociation in the presence of acid, metal cations or anions which bodes well for their use *in vivo*. The Ni(II) complex of **L3**, which is likely seven-coordinate, has very narrow proton resonances that give rise to a pronounced CEST peak. The other complexes are six-coordinate and show dynamic behavior on the NMR time scale that, while producing paraCEST, may lead to broadening of the peak. This shows that both the dynamic nature of the Ni(II) complexes and their coordination geometry are important in the development of the NiCEST approach.

■ ASSOCIATED CONTENT

Supporting Information

Materials and methods, synthesis, additional CEST and NMR spectra. This material is available free of charge via the Internet at http://pubs.acs.org.

■ AUTHOR INFORMATION

Corresponding Author

jmorrow@buffalo.edu

Notes

The authors declare no competing financial interest.

■ ACKNOWLEDGMENTS

We thank the Mark Diamond Research Fund of the Graduate Student Association at the University at Buffalo, the State University of New York and the John R. Oishei Foundation for support.

■ REFERENCES

(1) Viswanathan, S.; Kovacs, Z.; Green, K. N.; Ratnakar, S. J.; Sherry, A. D. *Chem. Rev.* **2010**, *110*, 2960.
(2) Dorazio, S. J.; Tsitovich, P. B.; Gardina, S. A.; Morrow, J. R. *J. Inorg. Biochem.* in press. DOI: 10.1016/j.jinorgbio.2012.06.007.
(3) Dorazio, S. J.; Tsitovich, P. B.; Siters, K. E.; Spernyak, J. A.; Morrow, J. R. *J. Am. Chem. Soc.* **2011**, *133*, 14154.
(4) Tsitovich, P. B.; Morrow, J. R. *Inorg. Chim. Acta in press,* 10.1016/j.ica.2012.06.010.
(5) *Comprehensive Coordination Chemistry*; Sacconi, L.; Mani, F.; Bencini, A., Eds.; Pergamon Press: Oxford, 1987; Vol. 5.
(6) Belle, C.; Bougault, C.; Averbuch, M.-T.; Durif, A.; Pierre, J.-L.; Latour, J.-M.; Le Pape, L. *J. Am. Chem. Soc.* **2001**, *123*, 8053.
(7) Bertini, I.; Luchinat, C. *NMR of Paramagnetic Molecules in Biological Systems*; Benjamin/Cummings Pub. Co.: Menlo Park, CA, 1986.
(8) La Mar, G. N. *J. Am. Chem. Soc.* **1965**, *87*, 3567.
(9) Roquette, P.; Maronna, A.; Reinmuth, M.; Kaifer, E.; Enders, M.; Himmel, H.-J. r. *Inorg. Chem.* **2011**, *50*, 1942.
(10) Weyhermuller, T.; Weighardt, K.; Chaudhuri, P. *J. Chem. Soc., Dalton Trans.* **1998**, 3805.
(11) Studer, M.; Riesen, A.; Kaden, T. A. *Helv. Chim. Acta* **1989**, *72*, 1253.
(12) Vaiana, L.; Regueiro-Figueroa, M.; Mato-Iglesias, M.; Platas-Iglesias, C.; Esteban-Gómez, D.; de Blas, A.; Rodríguez-Blas, T. *Inorg. Chem.* **2007**, *46*, 8271.
(13) Regueiro-Figueroa, M.; Esteban-Gómez, D.; Platas-Iglesias, C.; de Blas, A.; Rodríguez-Blas, T. *Eur. J. Inorg. Chem.* **2007**, *2007*, 2198.
(14) Dorazio, S. J.; Morrow, J. R. *Eur. J. Inorg. Chem.* **2012**, *2012*, 2006.
(15) Huang, C.-H.; Morrow, J. R. *Inorg. Chem.* **2009**, *48*, 7237.